



All Theses and Dissertations

---

2009-12-16

# Carbon Coated Tellurium for Optical Data Storage

Jonathan D. Abbott

*Brigham Young University - Provo*

Follow this and additional works at: <https://scholarsarchive.byu.edu/etd>

 Part of the [Astrophysics and Astronomy Commons](#), and the [Physics Commons](#)

---

## BYU ScholarsArchive Citation

Abbott, Jonathan D., "Carbon Coated Tellurium for Optical Data Storage" (2009). *All Theses and Dissertations*. 2360.  
<https://scholarsarchive.byu.edu/etd/2360>

This Thesis is brought to you for free and open access by BYU ScholarsArchive. It has been accepted for inclusion in All Theses and Dissertations by an authorized administrator of BYU ScholarsArchive. For more information, please contact [scholarsarchive@byu.edu](mailto:scholarsarchive@byu.edu), [ellen\\_amatangelo@byu.edu](mailto:ellen_amatangelo@byu.edu).

CARBON COATED TELLURIUM FOR OPTICAL DATA STORAGE

Jonathan Abbott

A thesis submitted to the faculty of  
Brigham Young University  
in partial fulfillment of the requirements for the degree of

Master of Science

Robert Davis  
Richard Vanfleet  
Matthew Linford

Department of Physics and Astronomy

Brigham Young University

April 2010

Copyright © 2010 Jonathan Abbott

All Rights Reserved

## ABSTRACT

### CARBON COATED TELLURIUM FOR OPTICAL DATA STORAGE

Jonathan Abbott

Department of Physics and Astronomy

Master of Science

A highly durable optical disk has been developed for data archiving. This optical disk uses tellurium as the write layer and carbon as a dielectric and oxidation prevention layer. The sandwich style CTeC film was deposited on polycarbonate and silicon substrates by plasma sputtering. These films were then characterized with SEM, TEM, EELS, ellipsometry, ToF-SIMS, etc, and were tested for writability and longevity. Results show the films were uniform in physical structure, are stable, and able to form permanent pits. Data was written to a disk and successfully read back in a commercial DVD drive.

Keywords: Archival, data storage, optical disk, tellurium

## ACKNOWLEDGMENTS

I would like to acknowledge the team at Millenniata, this has been a team project and would not have happened without everyone. The project was also funded by Millenniata, for which I am also grateful. Dr Davis and Vanfleet have offered as much support as be asked for, both in research and other ways, thank you. Lastly, and most importantly, I gratefully acknowledge the love and support of my wife and kids. We all share in this accomplishment.

# Contents

<b>Table of Contents</b>	<b>iv</b>
<b>List of Figures</b>	<b>v</b>
<b>1 Introduction</b>	<b>1</b>
1.1 Background . . . . .	2
1.2 Modeling . . . . .	3
1.3 Microscopy . . . . .	6
1.3.1 Atomic Force Microscopy . . . . .	6
1.3.2 Scanning Electron Microscope . . . . .	8
1.3.3 Transmission Electron Microscope . . . . .	10
<b>2 Experimental Work</b>	<b>11</b>
2.1 Methods and Materials . . . . .	11
2.2 Results . . . . .	13
2.3 Discussion . . . . .	20
<b>3 Conclusions</b>	<b>22</b>
3.1 Future Work . . . . .	22
<b>Bibliography</b>	<b>23</b>
<b>Index</b>	<b>25</b>

# List of Figures

1.1	Schematic representing the structure of the disk we have made. . . .	2
1.2	Model of CTeC stack for energy comparison before and after write . .	4
1.3	Delta E as a function of hole radius and carbon-tellurium interface energy	5
1.4	Schematic of AFM operation . . . . .	7
1.5	Schematic of SEM operation . . . . .	9
2.1	TEM characterization of films . . . . .	15
2.2	AFM and spectroscopic ellipsometry . . . . .	17
2.3	Characterization of pits . . . . .	18
2.4	Stability comparison . . . . .	19

# Chapter 1

## Introduction

In the last decade, significant progress has been made in data storage technology, both in capacity and speed. High capacity hard drives, flash memory, and Blu-ray optical disks are current examples of the continuing trend of higher capacities and faster seek times. One area that seems to have been neglected in all of these developments is the long term storage of digital data; by long term I mean storage for hundreds of years. Magnetic hard drives, flash memory, and current optical disk technologies are not appropriate for long term data storage because of their short data storage lifetimes [1] [2] [3] Currently paper is the best archival media available, but it is not suited for storing digital content (unless we go back to using punch cards).

In this thesis I present an archival optical disk using a novel carbon tellurium carbon (CTeC) sandwich as the write layer, see Fig 1.1 for a diagram. The carbon thin films were employed to protect the tellurium layer from oxidation-induced degradation. The CTeC sandwich write layer was prepared using plasma sputtering deposition and characterized with time of flight secondary ion mass spectrometry (ToF-SIMS) 3D analysis, AFM, TEM, and spectroscopic ellipsometry. SEM and optical microscopy were used to image the written marks, and a Pulstec ODU 1000 was

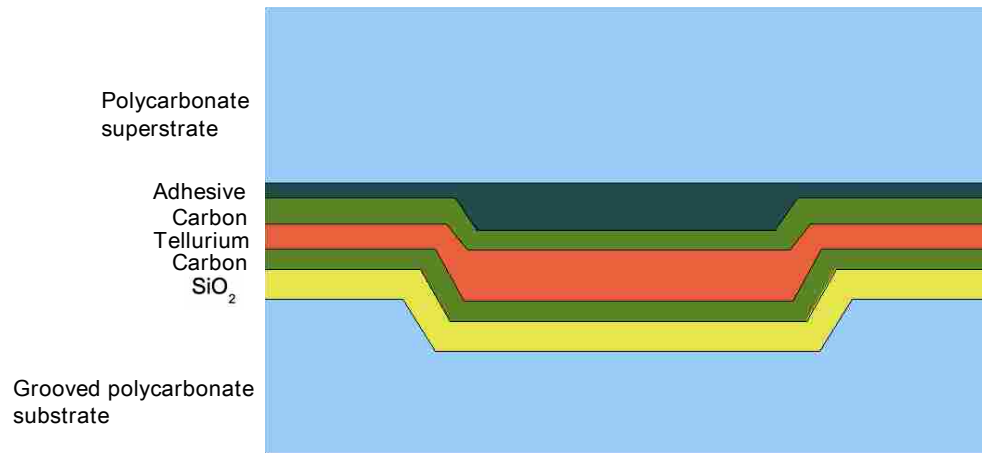


**Figure 1.1** Schematic representing the structure of the disc we have made.

used for writing and analysis of digital errors. Writing and lifetime expectancy tests show that permanent pits can be written to the CTeC based disks, and the disks are more resistant to degradation and subsequent data loss.

## 1.1 Background

While the disk structure I investigated is unique, tellurium has been studied as a write layer material before. At the time CD's were being developed, Terao et. al. investigated several materials as potential candidates for a write layer, including tellurium, lead, bismuth, tantalum and tin in addition to tellurium alloys AsTe and GeTe. [4] They found that in order to make clean holes in a material it was important that it have a high molten viscosity, it have high surface tension, the differences in melting points for alloy materials be small, the material have a uniform thickness, and that it not form large grains. The chalcogenides (group 16 elements) appeared to fit these requirements. Herd et. al. investigated holes in tellurium films with a top layer of carbon. [5]

Lou et. al. reported on a CD type disk that used tellurium as a write layer.

[6] They found that tellurium has adequate recording sensitivity and error rates. However, they found the expected lifetime of the disk to be about 10 years, based on a model presented by Milch and Tasaico. [7]

Kivits et. al. and later Suh et. al. investigated the hole formation process. [8] [9] Both groups found that simply melting the material in the laser spot was not sufficient to create a hole, that there was an energy barrier to overcome. These barriers are due to the surface energy change and the energy needed to overcome the inertial and viscous damping forces. If the hole to be formed is greater than a minimum radius, determined mainly by surface energy interactions, and the surface tension of the material is high enough a hole will be thermodynamically stable once formed.

## 1.2 Modeling

In order to investigate the energy barrier to hole formation in our material stack, I developed a simple model to find the difference in the surface energy before and after hole formation, illustrated in Fig 1.2. I assumed that the hole to be formed is cylindrical, and that after the hole is made there is no tellurium left on the carbon layers.

Before the hole is formed there are two carbon-tellurium interfaces that contribute to the surface energy difference. After the hole is formed those two carbon-tellurium interfaces become carbon-air interfaces. In addition, we now have a tellurium-air interface around the wall of the hole. The difference in the surface energy can now be written as

$$\Delta E = 2\pi r_o^2 (\gamma_C - \gamma_{C-Te}) + 2h\pi r_o \gamma_{Te}, \quad (1.1)$$

where  $h$  is the thickness of the carbon layer and  $r_o$  is the radius of the hole.  $\gamma_C$  is the surface energy of a carbon-air interface,  $\gamma_{Te}$  is the surface energy of the tellurium-air

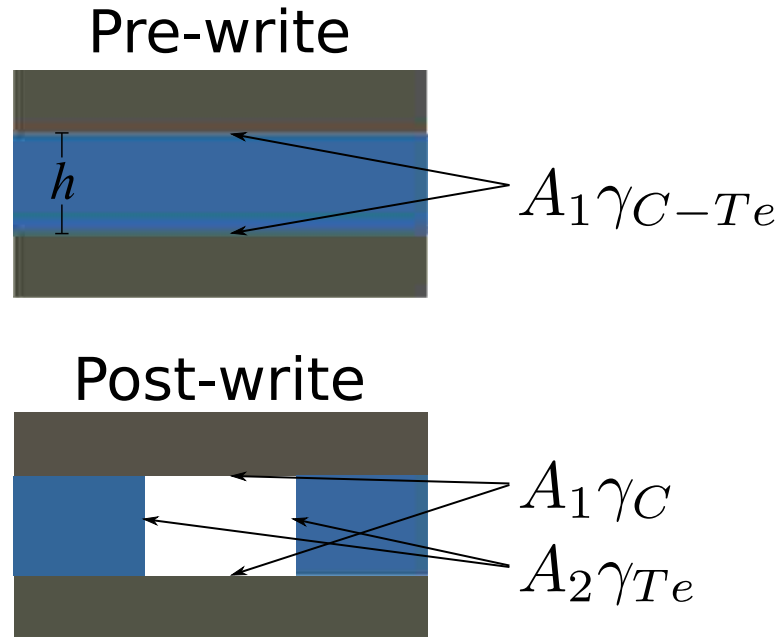


**Figure 1.2** Illustration of the simple model that was developed to compare the surface energy before and after forming a hole in the tellurium layer.

interface, and  $\gamma_{C-Te}$  is the surface energy of the carbon-tellurium interface. Using values from the literature [9] [10] I plotted equation (1.1), shown in Fig 1.3.

There are some interesting features to point out in Fig 1.3. First, there is a minimum hole size that must be reached before the hole will be stable thermodynamically. This is one of the barriers to hole formation that must be overcome. The minimum hole size depends on the interfacial energy of the carbon and tellurium layers. Second, as the radius of the hole gets larger the transition between stable and unstable holes gets sharper. This means that the write sensitivity, or how much power is required to begin making holes, can be tuned by varying the interfacial energy. This could be accomplished by doping the layers or otherwise changing the chemistry.

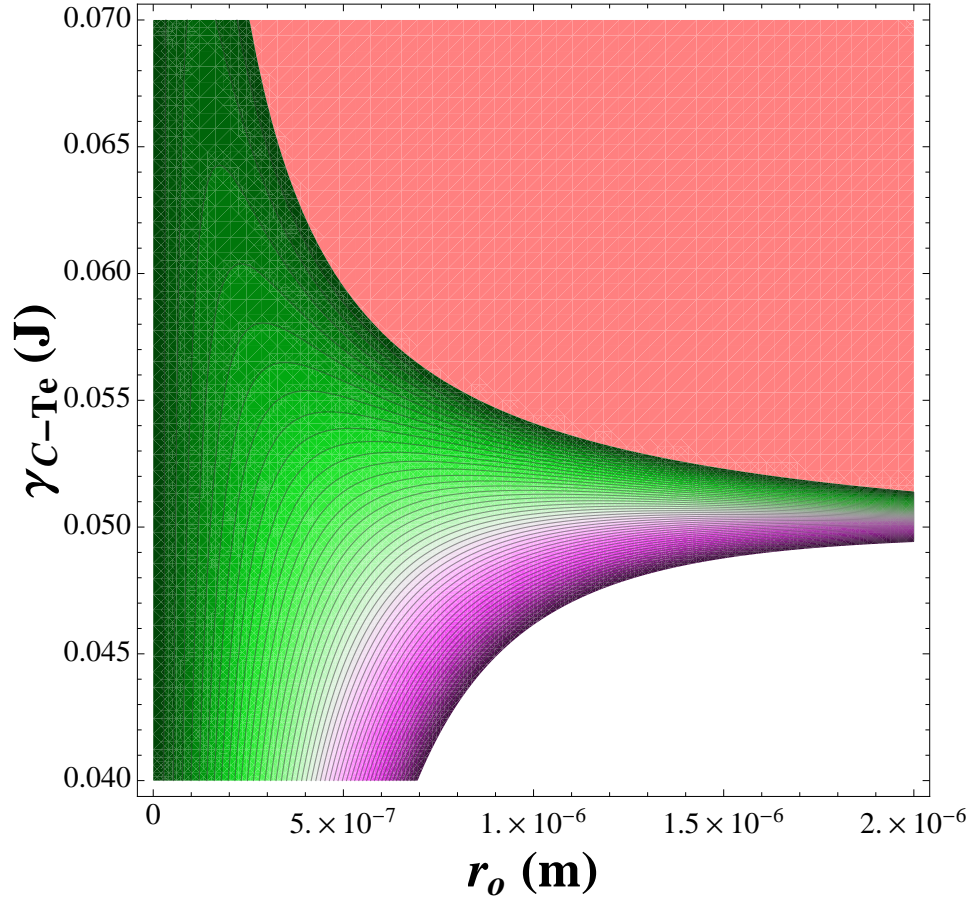


**Figure 1.3** The difference in surface energy before and after making a hole in the tellurium layer as a function of hole radius,  $r_o$ , and carbon-tellurium interface energy,  $\gamma_{C-Te}$ . The pink region is where  $\Delta E \leq 0$ , the white region is where  $\Delta E \geq 5 \times 10^{-14}$ .

## 1.3 Microscopy

In characterizing the CTeC stack I relied heavily on several different microscopy techniques. I will give a brief introduction to each of the instruments and techniques I used here to help those not already familiar with them. It is important to understand the capabilities and, perhaps more importantly, the limitations of each instrument and technique.

### 1.3.1 Atomic Force Microscopy

The AFM was invented in 1986 by Binnig, Quate, and Gerber as a result of collaboration between IBM and Stanford University. It overcame a serious limitation of the scanning tunneling microscope (STM), which was introduced several years earlier, in that it could image non-conductive surfaces where the STM could only image conducting or semi-conducting surfaces. Since then the AFM has been used to not only collect topographical data about a surface, but also probe magnetic fields, electric fields, hardness, friction, and more. It can be used in aqueous environments facilitating working with biological samples. It is a versatile instrument that has become a staple in many fields.

There are several different modes available on the AFM. In each mode a probe is scanned across a small area (some scanners allow up to 90  $\mu\text{m}$  on a side, many are limited to 10  $\mu\text{m}$  or less) by piezoelectric elements. The probe, or AFM tip, is typically made of silicon or silicon nitride. Fig ?? shows a typical AFM tip size and shape. Note how small the cantilever and tip are compared with the substrate they are attached to. The radius of the point at the end of the cantilever is usually around 10 nm. [11]

As the tip is scanned over a surface a laser is bounced off the back of the cantilever

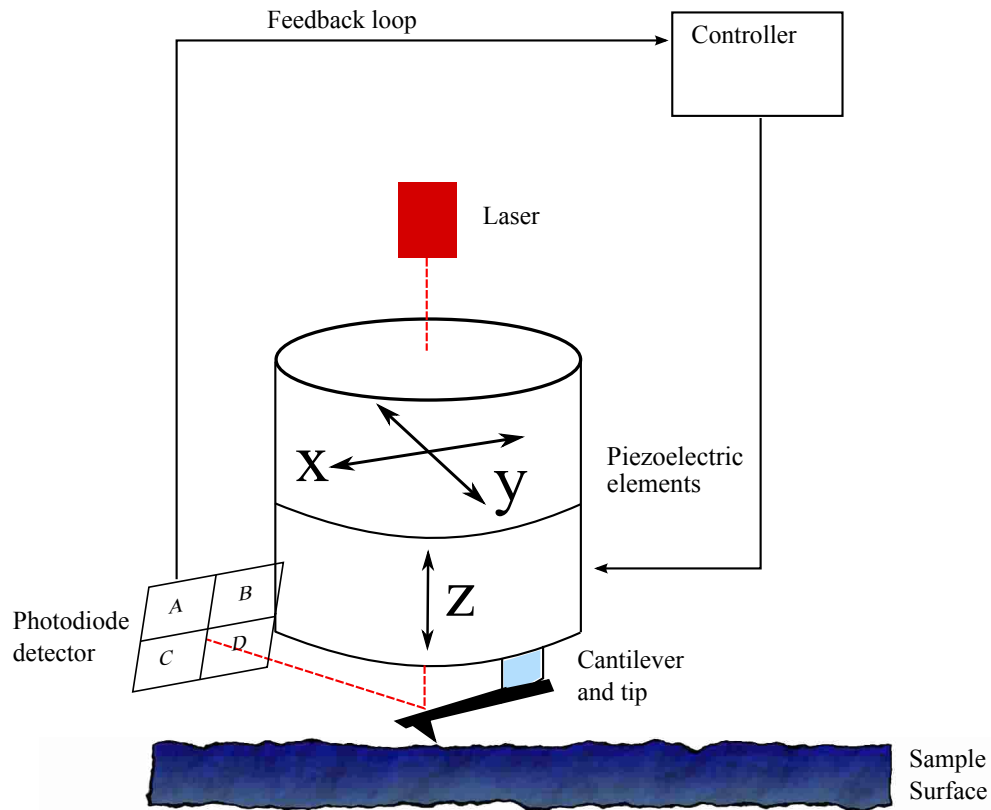


**Figure 1.4** Schematic of AFM operation.

on to a split photodiode detector. The photodiode detector is used to monitor either the deflection or oscillation frequency of the cantilever, depending on what mode the AFM is operated in. A schematic representation of the AFM is shown in Fig 1.4.

Contact mode is one of the most common modes to operate the AFM in. In this mode the tip is in contact with the surface to be imaged as it is scanned. A feedback loop maintains a constant cantilever deflection by moving the Z axis piezoelectric element up or down while the photodiode detector monitors the deflection. By maintaining a constant cantilever deflection the tip exerts a constant force on the sample, which can be adjusted by the user. An image is made by recording the position of the Z axis element at each x,y coordinate.

Tapping mode is the other commonly used mode for AFM. The cantilever is oscil-

lated at or slightly below its resonant frequency and the tip lightly 'taps' the surface being imaged. The feedback loop now maintains a constant oscillation amplitude by moving the Z axis piezoelectric element up or down to maintain a constant RMS of the oscillation signal measured by the photodiode detector. The image is made in the same way as for contact mode.

### 1.3.2 Scanning Electron Microscope

The first scanning electron microscope (SEM) was sold in 1965. SEM is used to take high resolution images of surfaces and can be used to gather elemental information about a sample with a back-scattered electron (BSE) or energy dispersive x-ray (EDX) detector. Because it uses electrons to form images instead of light, the SEM can achieve a resolution well beyond the diffraction limit of an optical microscope. The SEM can be used to image features from about 1 mm down to a few nanometers.

When an energetic beam of electrons hits the sample surface secondary, backscattered, and Auger electrons as well as characteristic x-rays are emitted from the surface. See Fig 1.5-a Typically the secondary electrons are used for imaging, while the backscattered electrons can give mass/thickness information, and the Auger electrons and x-rays are used for elemental analysis.

Care must be taken when preparing a sample for viewing in the SEM. Because it uses a beam of electrons for imaging, a non-conductive sample will charge up and make imaging impossible. The solution is to either sputter a conductive coating onto the surface (typically gold) or to use an environmental SEM (ESEM). The sample must also be high vacuum compatible. Many polymers and some inorganic materials have a vapor pressure that is too high. When you try to image these samples you may see beam induced deposition of whatever evaporated from the surface, mainly hydrocarbons, obscuring the surface you are trying to image and perhaps causing the

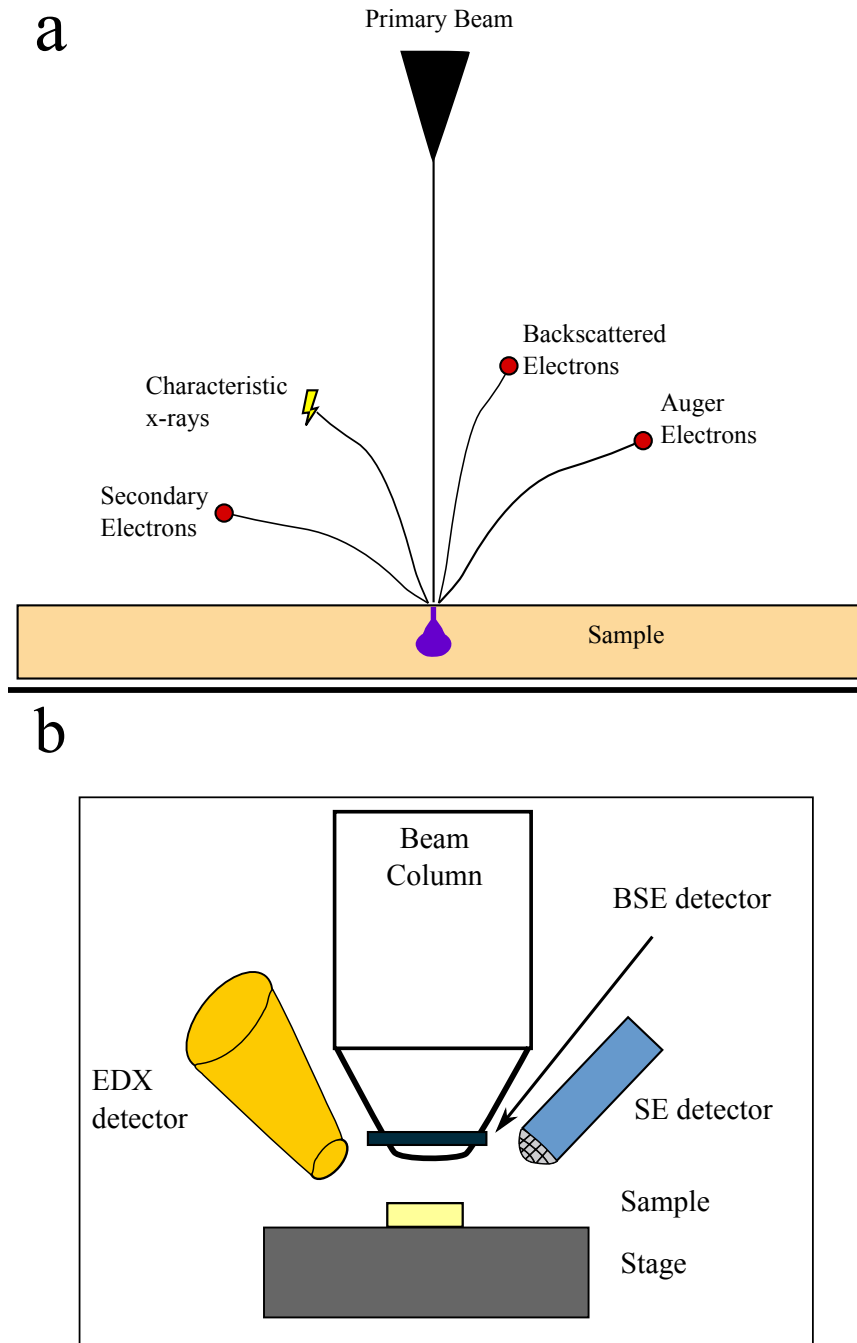


**Figure 1.5** a) Particles that are emitted from a sample when hit by an energetic electron beam. b) Schematic of the detectors available in a typical SEM

sample to charge up.

### 1.3.3 Transmission Electron Microscope

When the first transmission electron microscope (TEM) was being developed in 1932, it did not have any better resolution than a visible light microscope. Now it can be used to image columns of atoms in a crystalline sample. We can use the TEM to view images with several different contrast mechanisms, which each reveal different and complimentary information, as well as looking at diffraction patterns which reveal the crystal structure. In some instruments it is possible to do EDX (like in the SEM) and electron energy loss spectroscopy (EELS) and get elemental and chemical information about the sample. Doing this analysis in the TEM gives much higher spatial resolution for your elemental information than in the SEM.

In order to look at a sample in the TEM it must be thin. For good imaging the area of interest on the sample should be less than 100 nm thick, even thinner (>50 nm, the thinner the better) for good EELS spectra. There are several methods for creating these thin samples. Tripod polishing is a mechanical thinning method often used at BYU. Another method that is becoming more common at BYU is to use the focused ion beam (FIB) instrument. The FIB is an SEM with an ion gun that can be used for imaging, *in situ* deposition of some materials, and milling/cutting.

The TEM is capable of revealing a wealth of information about your sample, but with all that capability comes complication in operating the instrument and interpreting the results. There are many good books and textbooks devoted to all aspects of using the TEM, one place to start is with Transmission Electron Microscopy by Williams and Carter. [12]

# Chapter 2

## Experimental Work

In order to make a successful technical product it is important to understand how the materials used behave. If the properties are known and understood they can be manipulated to improve the product. The characterization presented in the following pages is not comprehensive, but it forms a basis for understanding what is happening in the disks.

### 2.1 Methods and Materials

The thin films used in this study were deposited in a PVD-75 system (Kurt J. Lesker) by reactive magnetron sputtering. The base pressure was  $10^{-5}$  Torr before deposition, the pressure rose to  $10^{-3}$  mTorr during deposition. Carbon was reactively sputtered from a 99.999% graphite target in an argon and carbon dioxide atmosphere at a power of 400 W. Tellurium was also reactively sputtered from a 99.999% elemental target in an argon and carbon dioxide atmosphere at a power of 20 W. The argon and carbon dioxide gases were 99.999% pure. Silicon dioxide was reactively sputtered from a 99.9999% elemental silicon target using 99.999% pure oxygen in argon. The carbon

layers were 13-20 nm thick, the tellurium layers 20-30 nm, and the silicon dioxide layer was 20-70 nm thick.

Film thicknesses were controlled by deposition time calibrated by AFM step height measurements. In order to get accurate step height measurements a marking pen lift-off technique was used to create the step edge in the deposited films. A line was drawn with a fine-tipped permanent marker (Sharpie) on a clean piece of silicon before depositing a film for a known time. After deposition the silicon substrate was rinsed in acetone to remove the permanent marker, then rinsed in isopropyl alcohol and deionized water. This process left a clean edge suitable for measuring film thickness.

Films were typically deposited onto grooved polycarbonate substrates 600  $\mu\text{m}$  thick, although some films were deposited onto silicon substrates. Prior to deposition, silicon substrates were cleaned with soap and water, rinsed in DI water, then dried with a jet of  $\text{N}_2$ . They were subsequently placed in an air plasma for 5 minutes. The polycarbonate was used as received from the manufacturer.

Writing was done with a Pulstec ODU 1000 system (Pulstec Industrial Co.,Ltd.). This system was used to develop the write strategy (tuning the laser pulse durations and powers), write data to the disks, and perform digital error analysis.

After deposition, the polycarbonate substrates were bonded to an un-grooved polycarbonate superstrate with a UV cure epoxy before writing with the ODU system. After writing, the top polycarbonate was removed. The exposed, written films were then imaged with SEM and AFM. To prepare a film for viewing in the TEM, a small piece was cut out of the substrate. The film on this small piece was lightly scratched with a scalpel into squares approximately 5 mm on a side. The piece was then placed in dichloroethane. When the film released from the substrate it was lifted out of the solvent with a 200 mesh copper TEM grid and was ready for viewing. The silicon substrates were used as deposited without further preparations.

ToF-SIMS data was collected using an IONTOF ToF-SIMS 5-100 system from ION-TOF GmbH. A 25 keV 0.25 pA Bi<sup>3+</sup> beam was used for the analysis and a 20 keV 0.25 nA C<sub>60</sub> beam was used for etching. Both beams had an incident angle of 45 deg. The etching was done over an area 300 μm X 300 μm, with the center 50 μm X 50 μm area used for analysis. Films for ToF-SIMS studies were deposited onto silicon substrates.

AFM data was collected on a Dimension V (Veeco) in tapping mode. SEM images were acquired in a Phillips XL S-FEG (FEI). TEM data was taken in a Technai F20 ASTEM (FEI).

Cross sections for viewing in the TEM were created in a Helios NanoLab 600 DualBeam system (FEI). A small piece was cut from the substrate, with the write layer that had been written to, and was mounted on a sample stub. The sample was coated with a thin ( 5-10 nm) layer of gold to reduce charging of the polycarbonate substrate. 50 nm of platinum was deposited in-situ with the electron beam to limit damage to the sample surface, after which 1 μm of platinum was deposited with the ion beam. A TEM sample was then cut, lifted out, attached to a half copper grid, and thinned for TEM viewing in-situ in the DualBeam chamber. The sample was then ready for TEM examination.

## 2.2 Results

The first characterization we present is of the physical structure of the layers. A focused ion beam (FIB) system was used to prepare a cross section sample. Fig 2.1-A shows the cross section viewed in the TEM in STEM mode. The top layer is a platinum layer deposited in the FIB as a protective layer. The bright layer is the tellurium, and the dark lines visible on either side of the tellurium are the carbon

layers. Under the bottom carbon layer the silicon dioxide layer is visible, under which is the polycarbonate substrate. EDX line scans of the cross section and ToF-SIMS 3D (Fig 2.1-E) both show that there was limited inter-diffusion of the deposited materials as indicated by relatively distinct boundaries between layers. The leading tail in the tellurium signal in Fig 2.1-E doesn't indicate interdiffusion at the carbon-tellurium interface, rather it is indicative of the faster ion etch rate for tellurium. For further discussion see Jiang et al. [13]

We also investigated the crystallinity of the deposited layers. Fig 2.1-B shows a bright field image of written marks taken by TEM. The brighter, oval areas in the image are the pits that were made during writing. A diffraction pattern was taken from an area in between the written marks, as indicated by the black box, using a 10  $\mu\text{m}$  selected area aperture. The diffraction pattern is shown in Fig 2.1-C, and appears to come from a single crystal grain of tellurium. The aperture diameter in the imaging plane was measured to be 190 nm. The tellurium layer is poly crystalline with an approximate grain size of at least 200 nm.

Electron energy loss spectroscopy (EELS) was used to investigate the crystallinity of the carbon layers, the results are shown in Fig 2.1-D as the solid line. Three reference spectra: graphitic, diamond-like, and amorphous carbon, are shown for comparison as dashed lines. While the intensities or heights of the peaks may vary, the general shape of the curve and/or peak ratios should not change significantly between similar materials. The spectrum obtained from our film has a small sharp peak at 285 eV, followed by a broad peak centered at about 296 eV. This matches well with the shape of the amorphous carbon spectrum, while the graphitic and diamond-like spectra both have features that are not seen in our spectrum. From this we conclude that the carbon layer in our films is amorphous.

AFM was used to measure film thicknesses on silicon substrates and obtain rough-

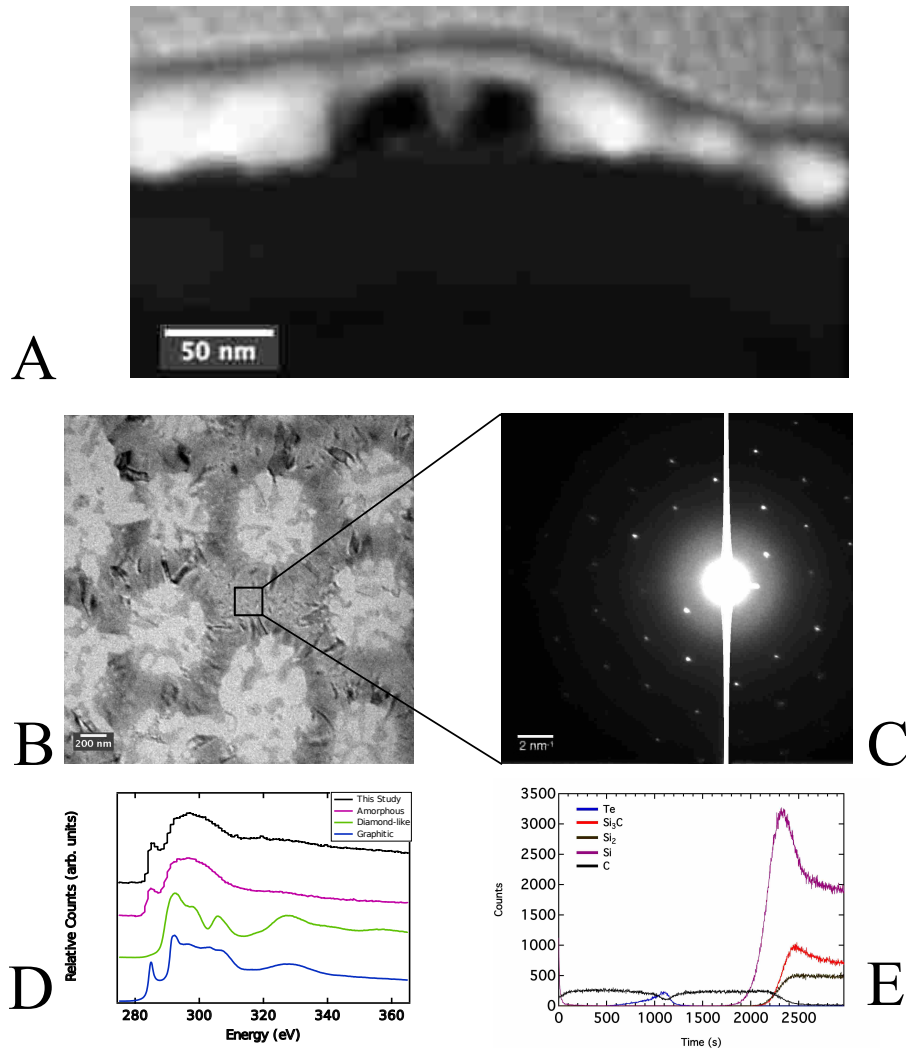


**Figure 2.1** Characterization of the write layer materials. A) STEM cross section of the write layer. The topmost layer is the platinum deposited to protect the surface, the bright middle layer is the tellurium, and the dark bands on either side of the tellurium are the carbon layers. The voids in the tellurium layer are written pits. B)-C) Bright-field TEM plan view of the write layer and a SAD pattern taken from the area highlighted by the box. The pattern appears to come from a single crystal grain. D) EELS spectra from the carbon layer.

ness data for our deposited films. The film thicknesses obtained from AFM measurements was used in determining the optical constants of our films using spectroscopic ellipsometry. Results of the AFM measurements and ellipsometry are shown in Figs 2.2-A thru F. Fig 2.2-A shows a tapping mode AFM image of a bare silicon substrate similar to the ones used in Figs 2.2-C and D. The roughness is 0.142 nm RMS. In Fig 2.2-B the optical constants for the individual carbon and tellurium films is plotted versus wavelength. In the last four images shown in Figs 2.2 (C - F) we investigated film roughness and used the step heights to determine deposition rates. Figs 2.2-C and D show the z-sensor image of the step edge for the tellurium and carbon films, respectively. Profiles were extracted and shown in Figs 2.2-D and F for the tellurium and carbon films, respectively.

In addition to investigating the layers themselves, the written marks were examined. The optical contrast can be seen in the HF trace shown in Fig 2.3-A, which shows the voltage on a photodiode while reading a disk in the ODU 1000 before removing the top dummy substrate. The contrast can also be seen in Fig 2.3-B, which is a reflected light optical micrograph taken after the dummy substrate was removed.

SEM and AFM were used to investigate the dimensions of the written marks. Fig 2.3-C shows an SEM image taken at normal incidence with a beam energy energy of 5 keV, using the TLD detector. The dark areas are the written pits, the bright flecks inside the pits are particles of tellurium that remained after the writing process. The bright rings around the pits are caused by a small accumulation of tellurium. Fig 2.3-D is a 10 X 10  $\mu\text{m}$  AFM image, collected in tapping mode, of the written pits. A profile was extracted from the line down the middle of the figure, along one of the data tracks and is shown in Fig 2.3-E. The horizontal line in Fig 2.3-E was placed by examining the unwritten areas in between marks, and indicates where the level of the unwritten film is.

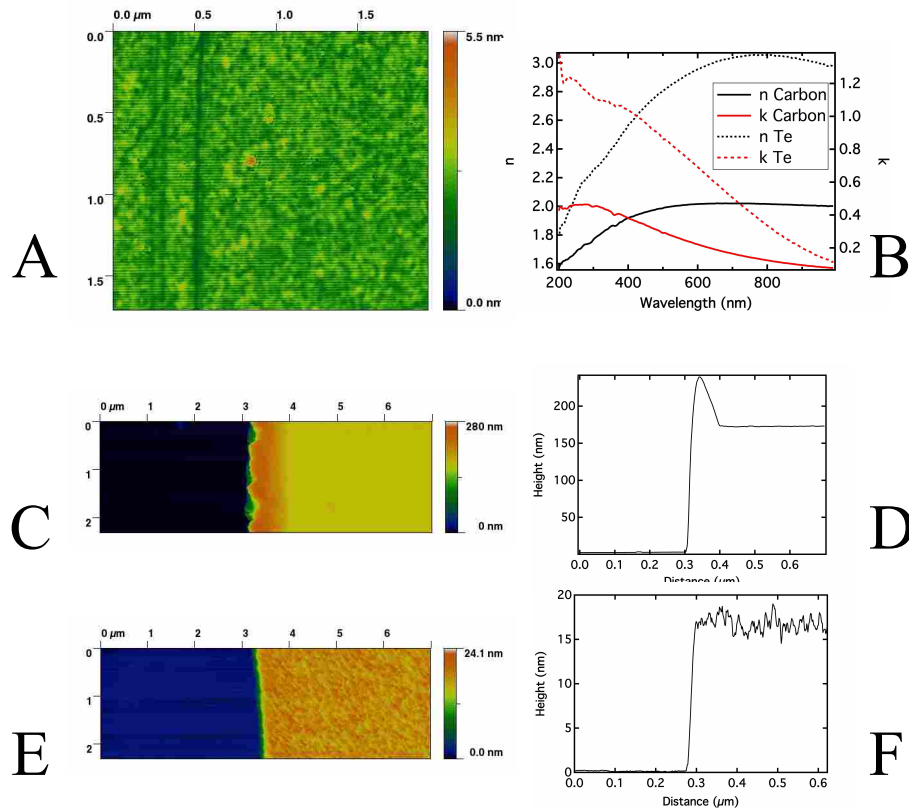


**Figure 2.2** AFM and ellipsometer analysis of the write layer. A) tapping mode AFM image of a piece of silicon wafer, similar to the ones used in C) and E). The roughness of the surface was measured to be  $1.4 \pm 0.5$  Å. B) Spectroscopic ellipsometer measurements of individual carbon and tellurium films. C) Tapping mode AFM image of a tellurium film step edge. The roughness of the film was  $7.9 \pm 0.3$  Å. D) Step edge profile of the tellurium film. E) Tapping mode AFM image of a carbon film step edge. The roughness of the film was  $5.2 \pm 0.1$  Å. F) Step edge profile of the carbon film.

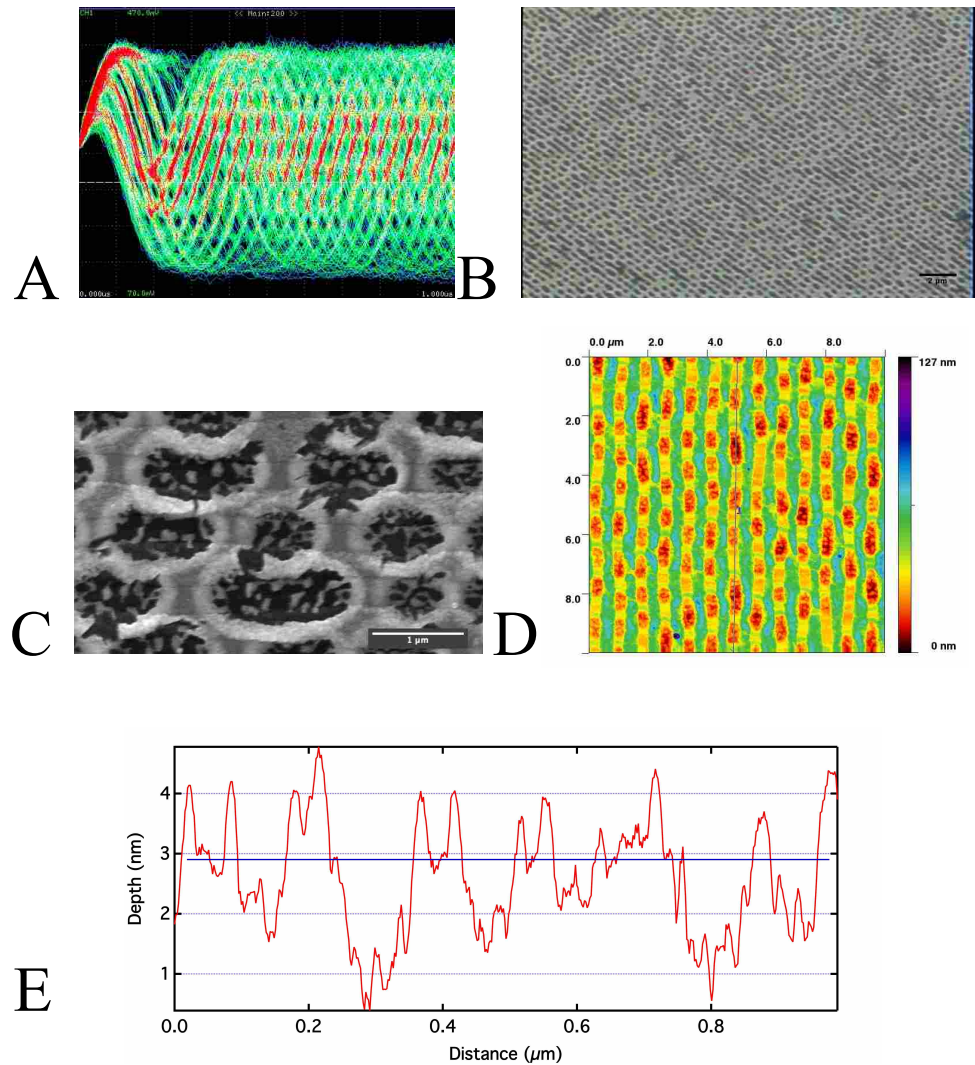


**Figure 2.3** Analysis of the written pits. A) HF trace showing the contrast between reflective lands and non-reflective pits for all the different sizes of pits superimposed. B) Optical micrograph of the written pits. C) SEM image of written pits. The bright rings around the pits are caused by an accumulation of material around them when the pits are written. D) Tapping mode AFM image of written pits. E) Profile taken along the line shown in D). The writing process forms pits in the write layer.

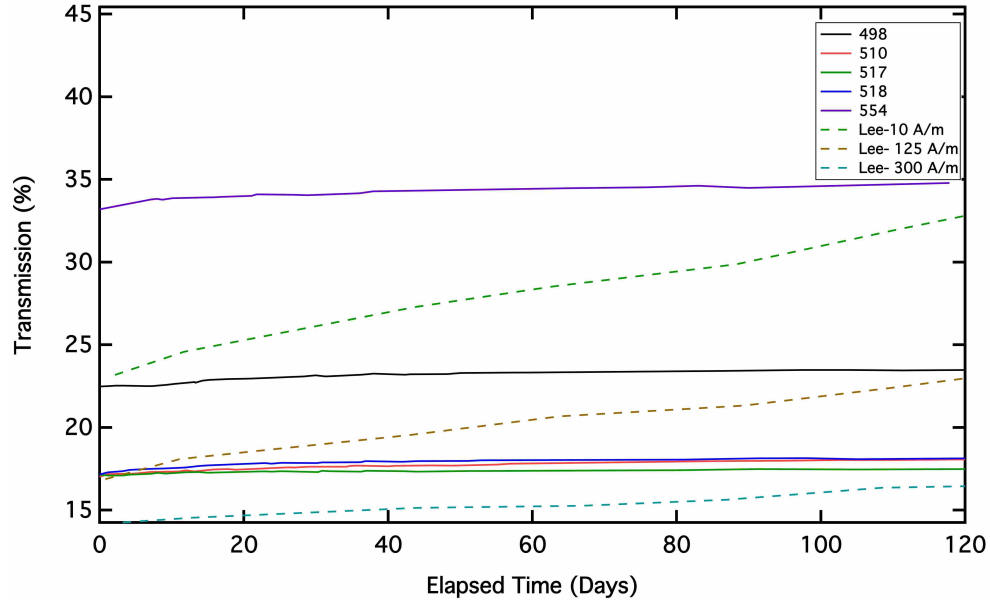


**Figure 2.4** Optical transmission of 5 different write layers were measured over 120 days at room temperature, shown in the solid lines. Optical transmission of bare tellurium films from Lee and Geiss is shown in the dashed lines for comparison.

To test the stability of the CTeC films, optical transmission was measured and compared to tellurium films without carbon. The solid lines in Fig 2.4 are CTeC films, the dashed lines are published tellurium films from Lee for comparison. [14]

Data to clock jitter is a measure of how well defined the pits and lands of a disk are [reference]. If the transition from pit to land or vice versa is not clean (sloped pit edge, jagged border, incorrectly formed pit, etc) it will result in a higher jitter value. The DVD specification states that the jitter can not be greater than 9% of a clock cycle; with a clock cycle of 38.32 ns data to clock jitter should not exceed 3.44 ns. [15] Table 2.1 lists average values for the data to clock jitter as well as average write power and reflectivity before write.

Parameter	Value
Write Power	$15.4 \pm 0.5$ mW
Data to Clock Jitter	$4.99 \pm 0.30$ ns
Reflectivity Before Write	$25.4 \pm 0.59\%$

**Table 2.1** Average values from 4 disks that were read in an off-the-shelf commercial drive. Reflectivity was measured with a wavelength of 650 nm.

## 2.3 Discussion

All of the disks included in table 2.1 were read back in commercial off-the-shelf drives. As seen in the optical micrograph in 2.2-B, the pits appear to be well defined in general. In the SEM and TEM images we saw that there were tellurium nano-particles that did not move during the write process, but those nano-particles did not appear to affect the optical contrast and our ability to read the data from the disks. As was mentioned previously, the bright rings around the pits are caused by a small accumulation of tellurium at the edges of the pits. The rings are visible in the AFM images in Figs 2.2-D and F. From Fig 2.2-F we can see that the rings are less than 5 nm tall and a few 10s of nanometers wide. These accumulation rings have been seen before in the literature (see references already given). It is possible that the rings of material contribute negatively to the jitter value; however, we were still able to read the data off the disks in an off the shelf commercial drive. The carbon layers do not negatively impact our ability to make pits in the tellurium.

The CTeC stack shows promise as a long term data storage layer. The optical transmission of the CTeC layer did not change appreciably after the 15 day point, while plain tellurium films showed 12% to 30% changes in transmission that continued after 120 days. Lee and Geiss saw a dependence of oxidation rate on the rate of film

---

deposition, with slower oxidation rates occurring with faster film depositions. [14] The CTeC films used in this study were deposited relatively slowly, 2 to 8 nm/min, so their oxidation rate cannot be attributed to fast deposition rates. Also, in previous work it was observed that the tellurium layer would oxidize locally at defects (rougher areas, scratches, etc) in the substrate. [16] The carbon film that the tellurium layer was deposited onto was seen to be very smooth, thus reducing the likelihood of oxidation of the tellurium layer.

# Chapter 3

## Conclusions

We have made a recordable DVD with a novel write layer consisting of layers of carbon and tellurium. The data on the recorded disks was readable on off the shelf drives. We have characterized the composition and structure of the layers and found that they represent a system with potential for long term stability, therefore this system shows promise as an archival data storage material.

### 3.1 Future Work

As was mentioned at the beginning of Chapter 2, the characterization presented here is not exhaustive and there is still more that could be learned about this stack. The better this stack is understood the the better we know how to improve it.

The model that was presented in the introduction was not very sophisticated, and I used values from the literature. The next step would be to improve the model by adding in a geometrical factor to make a more realistic approximation of the hole shape. Some effort would also be well spent in determining actual values for the surface energies of the materials in the disk. Because they are thin films and have

---

been sputtered with CO<sub>2</sub>, it is reasonable to expect that the surface energies will be different from the bulk tellurium or carbon. This would give a better representation of what is happening energetically in the disk during the write process. Coupling this with a calculation of the kinetics involved in hole formation would give a much fuller picture of hole formation in these disks and would help us understand what the effect of the carbon layers is. It would also lay the foundation of an experimental study of hole size as a function of surface energy.

Some other interesting questions that remain too are: does the tellurium stays in between the carbon layers during writing or does it get transported across the carbon layer, how well do the carbon layers retard the oxidation of the tellurium, and does the write process change the crystal structure or grain size of the tellurium. The answers to these questions would further our understanding of this stack of materials and provide insight into how to improve its performance.

# Bibliography

- [1] S. Dobrusina, S. Ganicheva, I. G. Tikhonova, T. D. Velikova, and P. E. Zavalishinb, “Influence of External Factors on the Longevity of Information Recorded on DVD  $\pm$  R Discs,” *Scientific and Technical Information Processing* **34**, 258–263 (2007).
- [2] O. Slattery, R. Lu, J. Zheng, F. Byers, and X. Tang, “Stability Comparison of Recordable Optical Discs-A Study of Error Rates in Harsh . . .,” *JOURNAL OF RESEARCH-NATIONAL INSTITUTE . . .* (2004).
- [3] J. S. Judge, R. G. Schmidt, R. D. Weiss, and G. Miller, “Media Stability and Life Expectancies of Magnetic Tape for Use with IBM 3590 and Digital Linear Tape Systems,” *20th IEEE / 11th NASA Goddard Conference on Mass Storage Systems and Technologies* (2003).
- [4] M. Terao, K. Shigematsu, M. Ojima, Y. Taniguchi, S. Horigome, and S. Yonezawa, “Chalcogenide thin films for laser-beam recordings by thermal creation of holes,” *JOURNAL OF APPLIED PHYSICS* **50**, 6881–6886 (1979).
- [5] S. Herd and K. Ahn, “Transmission electron microscopy for optical storage material analysis,” *Thin Solid Films* **108**, 341–351 (1983).

- 
- [6] D. Lou, G. Blom, and G. Kenney, "Bit oriented optical storage with thin tellurium films," *Journal of Vacuum Science and Technology* **18**, 78–86 (1981).
- [7] A. Milch and P. Tasaico, "STABILITY OF TELLURIUM FILMS IN MOIST AIR: A MODEL FOR ATMOSPHERIC CORROSION," *Journal of the Electrochemical Society* **127**, 884–891 (1980).
- [8] P. Kivits, R. Bont, B. Jacobs, and P. Zalm, "The hole formation process in tellurium layers for optical data storage," *Thin Solid Films* **87**, 215–231 (1982).
- [9] S. Suh, D. Snyder, and D. Anderson, "Writing process in ablative optical recording," *Applied Optics* **24**, 868–874 (1985).
- [10] A. Zebda, H. Sabbah, S. Ababou-Girard, F. Solal, and C. Godet, "Surface energy and hybridization studies of amorphous carbon surfaces," *Applied Surface Science* **254**, 4980–4991 (2008).
- [11] V. Instruments, *SPM Training Notebook*, rev. e ed., Veeco Instruments, 2003.
- [12] D. B. Williams and C. B. Carter, *Transmission Electron Microscopy* (Springer Science Business Media, LLC, 2009).
- [13] G. J. et al. (unpublished).
- [14] W.-Y. Lee and R. Geiss, "Degradation of thin tellurium films," *JOURNAL OF APPLIED PHYSICS* **54**, 1351–1357 (1983).
- [15] ECMA, "ECMA-267," ECMA (2001).
- [16] W.-Y. Lee, "The stability of thin tellurium and tellurium alloy films for optical data storage: II," *Thin Solid Films* **108**, 353–363 (1983).

# Index

Background,	2
Conclusions,	22
Discussion,	20
Experimental Work,	11
Future Work,	22
Methods and Materials,	11
Microscopy,	6
Atomic Force Microscopy,	6
Scanning Electron Microscope,	8
Transmission Electron Microscope,	10
Modeling,	3
Results,	13